臺北醫學大學 泌尿腎臟研究中心 會議紀錄

時間：**115 年 2 月 12 日(星期四) 09:30-11:00**

地點：視訊會議- (請以正式全名登入會議室，以利進行會議簽到)

使用 Google Meet (會議前 10 分鐘即開啟會議室)

會議室連結： https://meet.google.com/ihn-wugo-jfv

會議主席：吳美儀

與會人員：

【附醫】劉明哲、葉劭德、高治圻、吳建志、吳政誠、張景欣、方德昭、吳逸文、陳錫賢、江仰仁、陳靜怡、林彥仲、邵月珠、周安琪、吳致寬、李齊泰、林孝友、黃建榮、陳振文、陳寶寶、蔡東霖

【萬芳】溫玉清、李明哲、張渭文、林雍偉、蕭志豪、許軒豪、賴宗豪、鍾卓興、鄭仲益、陳作孝、劉崇德、楊韻紅、楊宇祥、李良明、林克勳、吳岳霖、廖宏偉

【雙和】李明哲、吳佳璋、陳冠州、劉家宏、江怡德、鄒凱亦、高偉棠、胡書維、吳美儀、洪麗玉、鄭彩梅、廖家德、宋睿祥、蔡旻光、陳佑瑋、高芷華、林冠宏、曾健華、邱伯涵、陳至亨、董劭偉、尹玉聰、林裕峯、宋立勤、柯玉誠、崔克宏

【北醫】羅偉成

【新國民】蘇裕謀、鄒居霖、江明傑、林宇璨、魏汶玲

長官指導：

吳麥斯校長、許志成教授、陳瑞明所長、盧星華副院長、許永和副院長

議程：

一、 特邀講師 — 台大醫院泌尿部 洪健華醫師

演講主題： Real-world study to translational research in prostate and urothelial diseases

二、 團隊報告

泌尿腎臟癌症團隊(劉家宏醫師)

三、 行政報告

1. 目前中心官網已委託廠商重新設計網站，若成員有相關績效亮點可協助提供，以利網站呈現（相關資料請 mail 至 25120@s.tmu.edu.tw 或傳至 RCUK 群組）。

2. RCUK 例會團隊報告順序（1 月至 7 月）

會議	時間	團隊
1月例會	1月29日(四)1130-1300	泌尿創新技術與手術團隊
2月例會	2月12日(四)0930-1100	腎臟泌尿團隊
3月例會	3月12日(四)1200-1330	急重症腎臟病照護團隊
4月例會	4月16日(四)1200-1330	慢性腎病整合照護團隊
5月例會	5月14日(四)1200-1330	功能性泌尿團隊
6月例會	6月17日(三)1200-1330	泌尿創新技術與手術團隊
7月例會	7月16日(四)1200-1330	腎臟泌尿團隊

3. **下次例會時間為 114 年 3 月 12 日 (四) 中午 12:00-13:00**

   外賓演講：由林雍偉主任邀請台大醫院邱士庭醫師至會議演講。

   團隊報告：急重症腎臟病照護團隊。(若需要協助播放簡報，煩請團隊最晚於會議前一日提供)

4. 目前中心共識營暫定 115 年 4 月 25 日(六)，再請各位成員預留時間參與，詳細資訊待確定後會公告於群組。

5. 往後成員若是有相關績效亮點、通過大型計畫、發表論文皆可於群組分享並提供相關資料，以利後續中心官網維護更新。

6. 請三院三科主任協助將尚未加入 LINE 群組的成員盡快加入群組，以利後續相關活動跟資訊公告。(目前群組 48 人含秘書，RCUK 成員共 72 人)


REAL-WORLD STUDY TO
TRANSLATIONAL RESEARCH IN
PROSTATE AND UROTHELIAL DISEASES
洪健華醫師
視訊會議連結：
https://reurl.cc/oYG4gV
現　職
台大醫院泌尿部
主治醫師
研究專長
一般泌尿學
攝護腺疾病
泌尿腫瘤
泌尿內視鏡與腹腔鏡微創手術
學　歷
國立臺灣大學醫學院
醫學系醫學士
醫學工程學系博士
經　歷
臺大醫院泌尿部總醫師
臺大癌醫中心分院
泌尿腫瘤外科兼任主治醫師
2/12 (四)
09:30-11:00

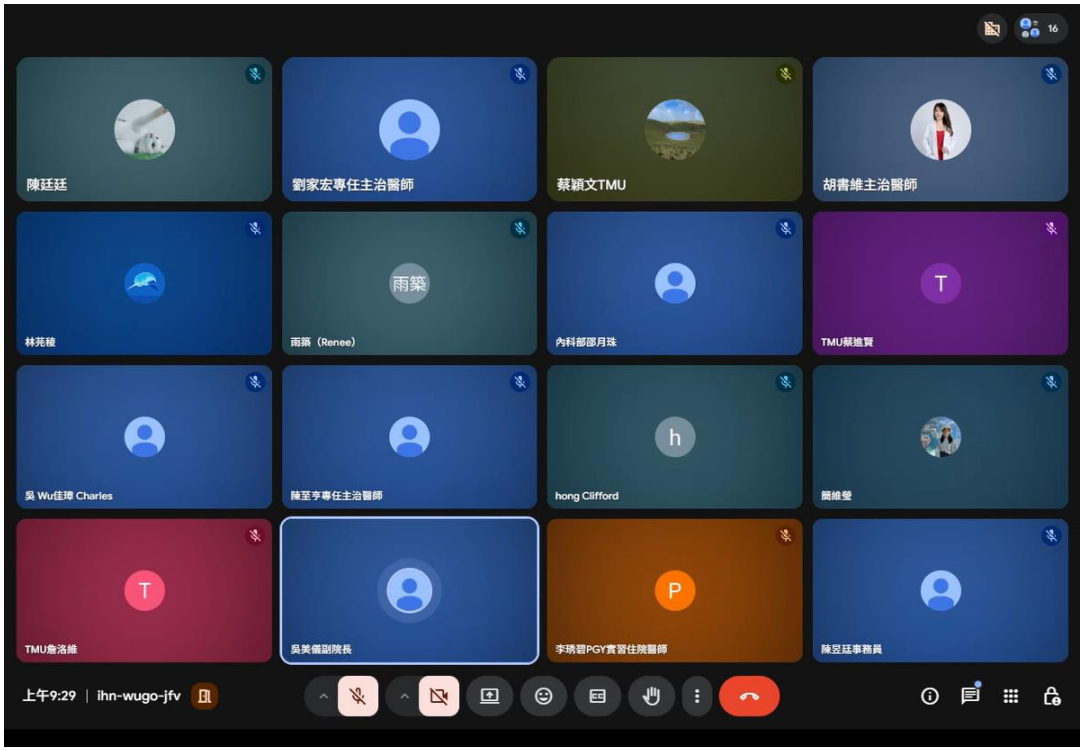
陳廷廷
劉家宏專任主治醫師
蔡穎文TMU
胡書維主治醫師
林芳穗
雨築 (Renee)
內科部邵月珠
TMU蔡進賢
吳 Wu佳珮 Charles
陳至亨專任主治醫師
hong Clifford
簡維瑩
TMU詹洛維
吳美儀副院長
李琇碧PGY實習住院醫師
陳昱廷事務員
上午9:29 | ihn-wugo-jfv

臺北醫學大學
TAIPEI MEDICAL UNIVERSITY

腎臟泌尿癌症團隊

Nano-orchestrated magnetotactic like navigation for electromagnetic theranostics and immune enhancement via photoautotrophic oxygenation, mild hyperthermia, and ferroptosis

報告人：劉家宏 醫師

Background-Bladder cancer

光合作用與磁性導航的雙重奏：克服腫瘤缺氧的奈米治療平台

基於小球藻 (Chlorella) 與與氧化鐵 (Iron Oxide) 的 CHL-GCS-IO 奈米系統

Modified Image from NoteBookLM

Background-Tumor Microenvironment

Modern Clinical Editorial

治療的瓶頸：缺氧的腫瘤微環境

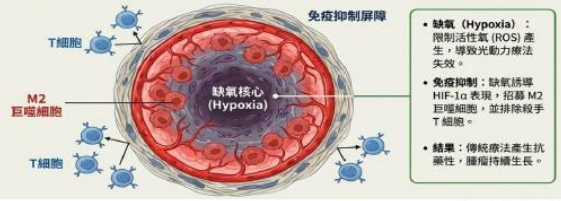

- **缺氧（Hypoxia）**：限制活性氧 (ROS) 產生，導致光動力療法失效。
- **免疫抑制**：缺氧誘導 HIF-1α 表現，招募 M2 巨噬細胞，並排除殺手 T 細胞。
- **結果**：傳統療法產生抗藥性，腫瘤持續生長。

Modified Image from NoteBookLM

Method and Meterials

Modern Clinical Editorial

解決方案：生物工程奈米平台

Modified Image from NoteBookLM

Method and Meterials

Modern Clinical Editorial

多重模態攻擊策略

協同效應：光合作用產生的氧氣直接增強了活性氧 (ROS) 的殺傷力。

Modified Image from NoteBookLM

Primary results

Materials analysis

Glycol chitosan - iron oxide Nanoparticles (GCS-IO NPs)

- Size： 230 nm ± 50 nm
- Zeta potential :
  - IO :-27.0 +- 1.06 mV
  - GCS-IO : 16.4 +- 0.76mV
- Spherical structure

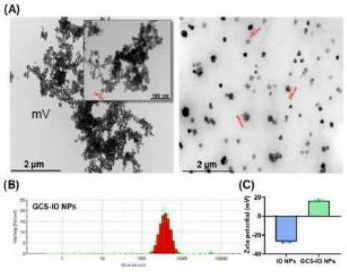

Primary results

Materials analysis

Glycol chitosan - iron oxide Nanoparticles (GCS-IO NPs)

- FTIR spectra of GCS, IO NPs, and GCS-IO NP : the presence of Fe-O bond
- XRD patterns of GCS, IO NPs, and GCS-IO NPs :crystalline structure of IO in GCS-IO NPs
- SQUID : GCS-IO NPs exhibited suitable for magnetic targeting applications

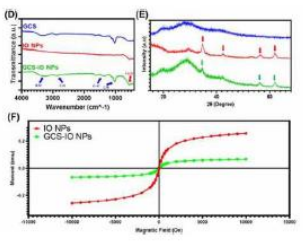

Primary results

Materials analysis

Glycol chitosan - iron oxide Nanoparticles (GCS-IO NPs)

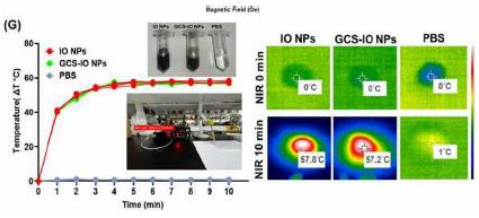

Primary results

Materials analysis

Chlorella-Glycol chitosan - iron oxide Nanoparticles (CHL-GCS-IO NPs)

- a time- and concentration-dependent increase in oxygen production, with high reactive oxygen species (ROS) generation tendency at higher NP concentrations and longer irradiation times
- CHL-GCS-IO NPs exhibited higher fluorescence intensities, indicating enhanced oxygen generation
- + 10 mV for CHL-GCS-IO NPs suggests successful conjugation of GCS-IO NPs and improved colloidal stability

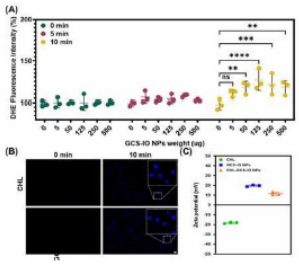

Primary results

Materials analysis

Chlorella-Glycol chitosan - iron oxide Nanoparticles (CHL-GCS-IO NPs)

The merged image confirms successful conjugation, with distinct fluorescent signals for FITC and chlorophyll.
CHL-GCS-IO NPs demonstrated slightly increased chlorophyll activity compared to untreated CHL
RDPP data of CHL and CHL-GCS-IO NPs evaluated at 0 min and 10 min light irradiation

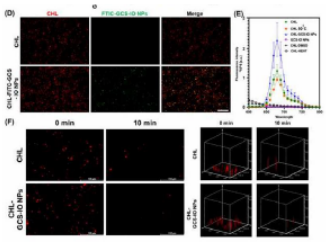

Primary results

Materials analysis

Chlorella-Glycol chitosan - iron oxide Nanoparticles (CHL-GCS-IO NPs)

- SEM of shows CHL-GCS-IO NPs exhibit surface roughness,
- EDS demonstrates a significant increase in iron (Fe), confirming NP attachment
- FTIR shows characteristic peaks of C = O stretching (~ 1700 cm⁻¹), C-N stretching (~ 1400 cm⁻¹), and Fe-O (~ 600 cm⁻¹), confirming successful conjugation and preservation of bioactivity.
- XRD showed CHL-GCS-IO NPs, confirming the incorporation of magnetic NPs into the Chlorella system

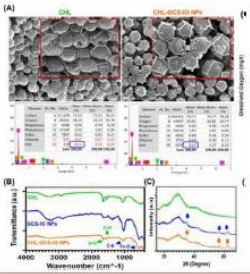

Primary results

Materials analysis

Chlorella-Glycol chitosan - iron oxide Nanoparticles (CHL-GCS-IO NPs)

1.CHL-GCS-IO highlighting their potential for PTT
2. SQUID showed CHL-GCS-IO NPs indicates superparamagnetic behavior with significantly higher saturation magnetization
3. T2-weighted magnetic resonance imaging (MRI) analysis: CHL-GCS-IO NPs demonstrated strong T2 contrast, enhancing their potential as MRI contrast agents for precise tumor imaging in theranostic applications.

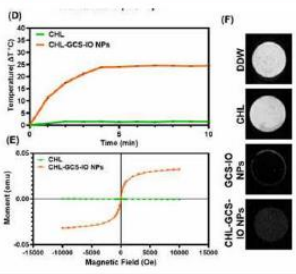

Primary results

Materials analysis Chlorella-Glycol chitosan - iron oxide Nanoparticles (CHL-GCS-IO NPs)

CHL-GCS-IO NPs exhibit significantly enhanced oxygen production compared to CHL, indicating improved photosynthetic efficiency

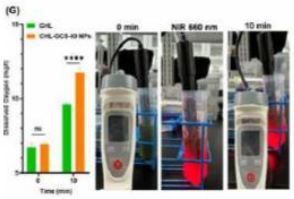

Primary results

Materials analysis Chlorella-Glycol chitosan - iron oxide Nanoparticles (CHL-GCS-IO NPs)

Electromagnetic wave responses of Chlorella (CHL) and CHL-GCS-IO NPs under light irradiation. The electromagnetic field (E-field) measurements demonstrate a negligible change in CHL samples under light exposure, while CHL-GCS-IO NPs exhibit a substantial increase in electromagnetic activity, likely attributed to the conductive and electromagnetic-responsive properties of the glycol iron oxide nanoparticle

Primary results

MB49-Cell viability Chlorella-Glycol chitosan - iron oxide Nanoparticles (CHL-GCS-IO NPs)

Both CHL and CHL-GCS-IO NPs exhibited moderate cytotoxicity, with cell viability remaining above 60% (0–100 µg/mL).

CHL-GCS-IO NPs, when irradiated with 660- and 808 nm-light, resulted in a significant decrease in cell viability (~ 70% cell death).

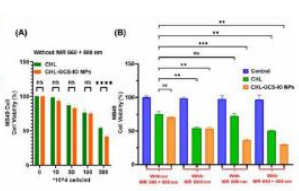

Primary results

MB49 cell-ROS generstion Chlorella-Glycol chitosan - iron oxide Nanoparticles (CHL-GCS-IO NPs)

DCFH-DA assay :The CHL-GCS-IO NPs group exhibited significantly higher ROS generation than CHL alone, and the addition of H_2O_2 further amplified ROS production.

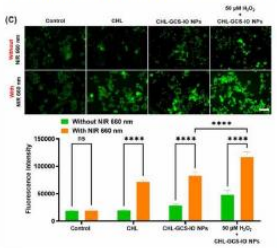

Primary results

MB49 cell-ROS generstion Chlorella-Glycol chitosan - iron oxide Nanoparticles (CHL-GCS-IO NPs)

DCFH-DA assay :The CHL-GCS-IO NPs group exhibited significantly higher ROS generation than CHL alone, and the addition of H_2O_2 further amplified ROS production.

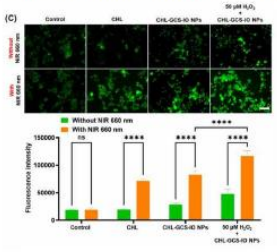

Primary results

MB49 cell - Ferroptosis Chlorella-Glycol chitosan - iron oxide Nanoparticles (CHL-GCS-IO NPs)

CHL-GCS-IO NPs significantly induce iron accumulation in MB49 cells, as evidenced by Prussian blue staining, compared to control and CHL only treatments. This effective delivery of iron oxide nanoparticles through Chlorella likely initiates ferroptosis, a form of programmed cell death linked to lipid peroxidation.

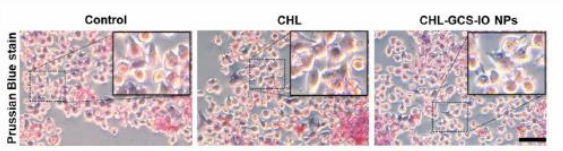

Primary results

Polarization of RAW264.7 macrophages : M0-M1 Chlorella-Glycol chitosan - iron oxide Nanoparticles (CHL-GCS-IO NPs)

Quantitative analysis of the fluorescence intensity, using ImageJ software, confirmed the significant increase in CD86 expression by CHL-GCS-IO NPs under NIR irradiation

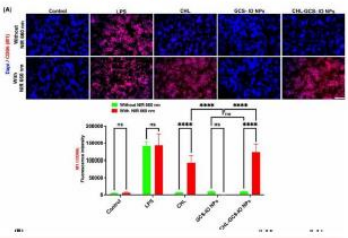

Primary results

Polarization of RAW264.7 macrophages : M2-M1 Chlorella-Glycol chitosan - iron oxide Nanoparticles (CHL-GCS-IO NPs)

(M2 to M1 re-polarization (CD206 to CD86 expression shift). IL-4 (an M2 polarization inducer) :Quantitative analysis using ImageJ software demonstrated a significant increase in CD86 and a decrease in CD206 expression after NIR irradiation in the CHL-GCS-IO NP group

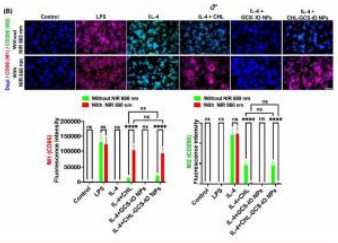

Primary results

Animal experiments Chlorella-Glycol chitosan - iron oxide Nanoparticles (CHL-GCS-IO NPs)

MB49 tumor cell injection, formulations administration, near infrared (NIR) irradiation, and tumor size monitoring.
This image was created and edited using BioRender software

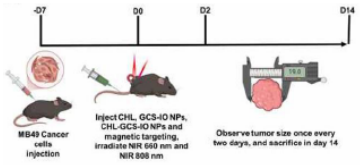

Primary results

Animal experiments,

Chlorella-Glycol chitosan - iron oxide Nanoparticles (CHL-GCS-IO NPs)

- After 1 hr : A quantitative analysis indicated a significant increase in tumor accumulation by CHL-GCS-IO NPs in the magnetic-targeted group compared to the other groups
- After 7 days:Fluorescence imaging demonstrated clearance of the formulations, with a residual signal observed in the tumor of CHL-GCS-IO NPs of the magnetic-targeted group . A quantitative analysis showed significantly higher retention in the tumor by
- magnetically targeted CHL-GCS-IO NPs.

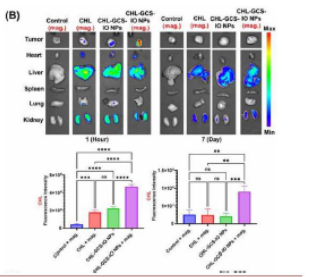

Primary results

Animal experiments,

Chlorella-Glycol chitosan - iron oxide Nanoparticles (CHL-GCS-IO NPs)

- Infrared thermal imaging of MB49 tumor-bearing mice subjected to 808-nm NIR irradiation for 5 min.
- Images reveal a significant temperature rise in the GCS-IO NPs and CHL-GCS-IO NPs groups, with CHL-GCS-IO NPs (magnetic) reaching the highest temperature (~ 50.8 °C), indicating a strong photothermal conversion efficacy

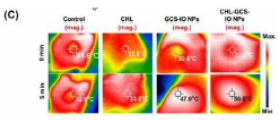

Primary results

Animal experiments,

Chlorella-Glycol chitosan - iron oxide Nanoparticles (CHL-GCS-IO NPs)

MB49 tumor-bearing mice treated with control, CHL, GCS-IO NPs, and CHL-GCS-IO NPs over a 14-day period.
Tumor sizes were monitored and photographed every 2 days following intravenous administration of the formulations and subsequent magnetic targeting, and NIR 660- and 808-nm irradiation.
Quantitative tumor growth curves for each group, normalized to the day 0 tumor size, are shown in the bottom panel. Data are presented as mean ± SD (n = 5).

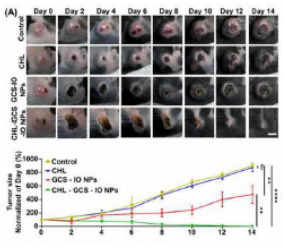

Primary results

Animal experiments,

Chlorella-Glycol chitosan - iron oxide Nanoparticles (CHL-GCS-IO NPs)

Ex vivo images of excised tumors from all treatment groups after sacrifice on day 14. The tumor size and appearance visibly decreased in the GCS-IO NPs and CHL-GCS-IO NPs groups compared =to the control and CHL groups, with the smallest tumor masses observed in the CHL-GCS-IO NPs group
Quantitative analysis of sizes of excised tumors from all groups, normalized to control group's tumor size.

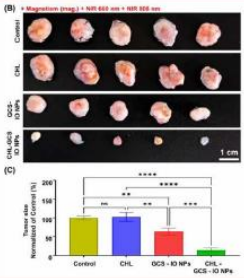

25

Primary results

Animal experiments,

Chlorella-Glycol chitosan - iron oxide Nanoparticles (CHL-GCS-IO NPs)

Hypoxia-inducible factor (HIF)-1α staining (yellow). a marker of hypoxia, Quantification of the fluorescence intensity revealed significant downregulation of HIF-1α in the CHL-GCS-IO NPs group

C-X-C Motif Chemokine Ligand 12 (CXCL12) (purple). IF images showed CXCL12 expression, a factor linked to tumor metastasis and angiogenesis.Quantification indicated significant downregulation in the CHL-GCS-IO NPs group

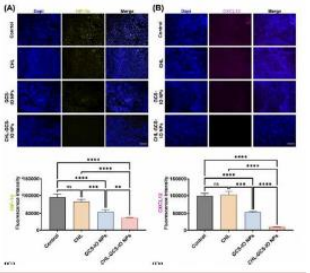

26

Primary results

Animal experiments,

Chlorella-Glycol chitosan - iron oxide Nanoparticles (CHL-GCS-IO NPs)

Transforming growth factor (TGF)-β staining (green), a cytokine involved in immune suppression and tumor metastasis.
Quantification confirmed significant downregulation of TGF-β in the CHL-GCS-IO NPs group
Amplex red staining (red). Detection of reactive oxygen species (ROS) via Amplex red staining. A quantitative analysis confirmed significantly higher ROS production in the CHL-GCS-IO NPs group.

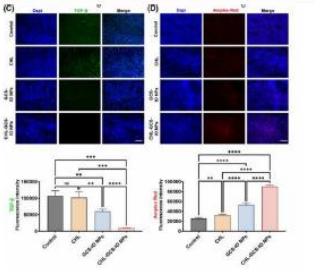

27

Primary results

Animal experiments,

Chlorella-Glycol chitosan - iron oxide Nanoparticles (CHL-GCS-IO NPs)

Programmed death ligand 1 (PD-L1) expression. PD-L1 IF staining (purple). A quantitative analysis confirmed significantly lower PD-L1 levels in the CHL-GCS-IO NPs group compared to all other groups

Cluster of differentiation 11c (CD11c) expression (dendritic cells (DCs)). CD11c IF staining (red) in tumor tissues indicated enhanced DC activation in the GCS-IO NPs group, with the highest activation seen in the CHL-GCS-IO NPs group

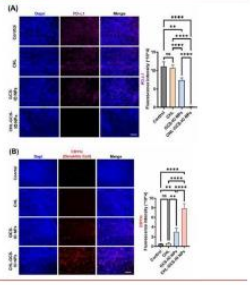

28

Primary results

Animal experiments,

Chlorella-Glycol chitosan - iron oxide Nanoparticles (CHL-GCS-IO NPs)

CD49b expression (natural killer (NK) cells). CD49b IF staining (green) revealed increased NK cell recruitment and activation, particularly in the CHL-GCS-IO NPs group, where the highest expression of CD49b was observed

CD8+ T-cell infiltration. CD8+ IF staining (green) showed robust T-cell infiltration in the CHL-GCS-IO NPs group, with significantly higher CD8+ levels compared to all other groups.

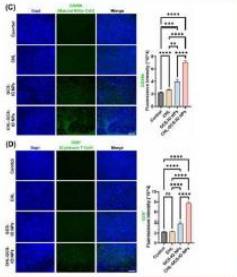

29

Primary results

Animal experiments, Chlorella-Glycol chitosan - iron oxide Nanoparticle (CHL-GCS-IO NPs)

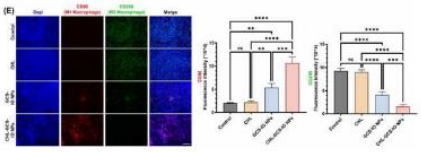

Macrophage polarization. CD86 (M1 macrophages, red) and CD206 (M2 macrophages, green) staining showed a marked shift toward proinflammatory M1 polarization in the CHL-GCS-IO NPs group, with a significant increase in CD86 and a corresponding decrease in CD206 expression.

30

Conclusion

This study introduces a translational system of nano-orchestrated magnetotactic like system, integrating photosynthetic oxygenation, remote hyperthermia, and ferroptosis to achieve comprehensive tumor eradication and immune activation. The CHL enhanced oxygen production by continuously alleviating hypoxia, boosting both electromagnetic therapeutic efficacies and ferroptosis-induced tumor cell death. Moreover, the multimodal CHL-GCS-IO NPs reprogrammed the TME, facilitating immune activation by promoting macrophage polarization towards the proinflammatory M1 phenotype, engaging cytotoxic T cells and natural killer cells, programmed death ligand 1 (PD-L1) downregulation, and driving dendritic cell reprogramming towards improved antigen presentation.

31

Thank you for listening!

32